The Journal of Antibiotics (2018) 71:1018–1024
https://doi.org/10.1038/s41429-018-0096-1

JARA Japan Antibiotics Research Association
The Society for Actinomycetes Japan

ARTICLE

Cytotoxic antibiotic angucyclines and actinomycins from the *Streptomyces* sp. XZHG99T

Jie Bao[1] · Fei He[1] · Yumei Li[1] · Lei Fang[1] · Kaiming Wang[1] · Jintong Song[1] · Jie Zhou[1] · Qiang Li[1] · Hua Zhang[1]

Received: 20 May 2018 / Revised: 3 August 2018 / Accepted: 9 August 2018 / Published online: 29 August 2018

Abstract

Three new angucycline-type *C*-glycosides, grincamycins L–N (**1**–**3**), together with the known rabelomycin (**4**), moromycin B (**5**), fridamycin D (**6**), saquayamycin B1 (**7**), actinomycin X_2 (**8**), and actinomycin D (**9**), were isolated from the culture of the soil-derived *Streptomyces* sp. XZHG99T collected from Color desert, Dengpa District, Tibet. The structures of **1**–**3** were established by detailed analyses of comprehensive spectroscopic data. Compounds **1**–**9** exhibited significant cytotoxicity against a panel of human cancer cell lines A549, H157, MCF7, MDA-MB-231, and HepG2, while **4**, **8**, and **9** showed decent antibacterial activity against *Mycobacterium smegmatis* and *Staphylococcus aureus*.

Introduction

Antimicrobial resistance (AMR) has become a major threat to the global public health especially in developing countries and it is anticipated to be responsible for 10 million death cases every year and a reduction of 2 to 3.5% in Gross Domestic Product (GDP) by 2050 [1]. Therefore, the development of new types of antibiotics against microbe-related diseases remains an urgent requirement. Among all antibiotic-producing microbes, the *Streptomyces* species are considered to be the most important resource and account for the production of 50–55% known antibiotics [2, 3]. Angucyclines and actinomycins are two classes of important antibiotics produced by *Streptomyces* sp., with a broad spectrum of biological properties especially anticancer and antibacterial activities [4–7]. Angucyclines are characterized in the tetracyclic benz[a]anthracene core and most of them exist as *O*- or *C*- glycosides in nature. Actinomycins are a family of chromopeptide lactones, and as the most well-known member of them, actinomycin D has been widely used in clinic as an anti-tumor drug for the treatment of childhood rhabdomyosarcoma and Wilms' tumor [5, 6]. Meanwhile, actinomycin D also exhibited excellent activity against gram-positive bacteria [5, 6].

As a continuation of our effort to discover new antibacterial agents from actinomycetes based on a bioassay-guided strategy, the *Streptomyces* sp. XZHG99T from the soil sample collected from Color desert, Dengpa District, Tibet (29°66′ N, 84°55′ E) showed well inhibitory activity against *Staphylococcus aureu*. Our investigation on the crude extract led to the isolation and identification of three new angucycline-type derivatives grincamycins L–N (**1**–**3**), four structurally related co-metabolites including rabelomycin (**4**) [8, 9], moromycin B (**5**) [10], fridamycin D (**6**) [11] and saquayamycin B1 (**7**) [12], and two actinomycin analogs actinomycin X_2 (**8**) [5] and actinomycin D (**9**) [5] (Fig. 1). Grincamycin L was the first example of angucycline family having a rhodinosyl *C*-glycoside linkage at C-9, implying the likely participation of a specific glycosyltransferase in the biosynthetic process. Herein we reported the isolation, structure elucidation and bioactivity of compounds **1**–**9**.

Results and discussion

Grincamycin L (**1**) was isolated as a yellow powder, and the molecular formula was determined to be $C_{31}H_{30}O_{10}$ based on the HR-ESIMS ion at *m/z* 561.1764 $[M-H]^-$(calcd for $C_{31}H_{29}O_{10}$, 561.1766). An anthraquinone skeleton was

Electronic supplementary material The online version of this article (https://doi.org/10.1038/s41429-018-0096-1) contains supplementary material, which is available to authorized users.

✉ Hua Zhang
bio_zhangh@ujn.edu.cn

[1] School of Biological Science and Technology, University of Jinan, 336 West Road of Nan Xinzhuang, Jinan 250022, China

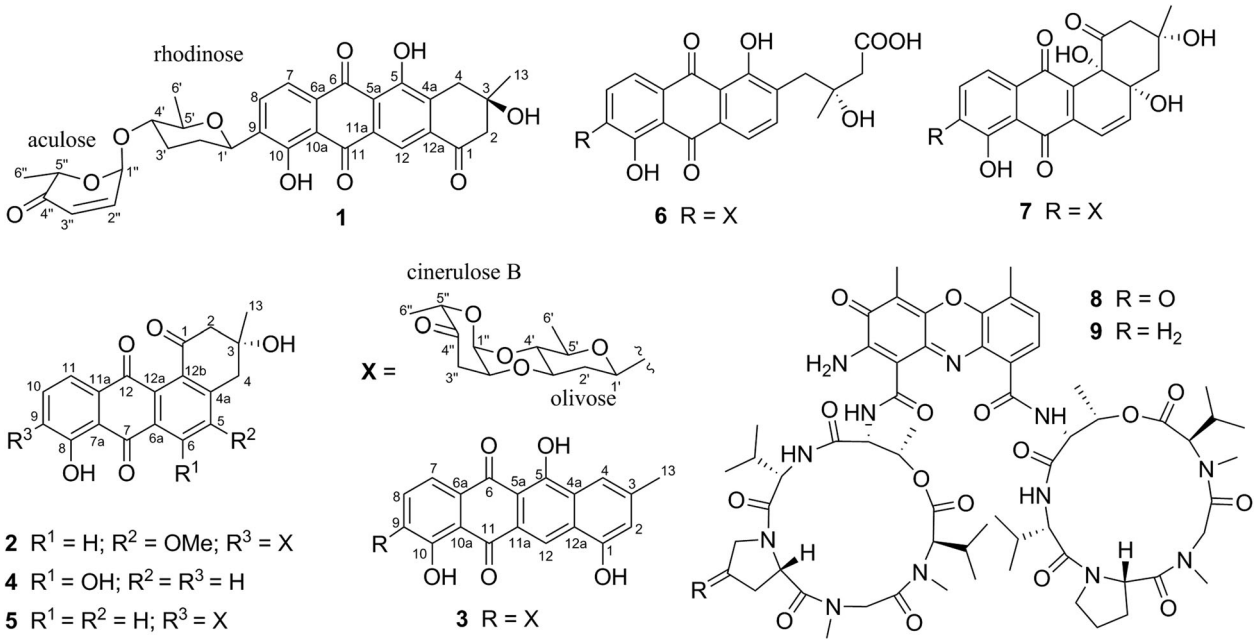

Fig. 1 Chemical structures for compounds **1**–**9**

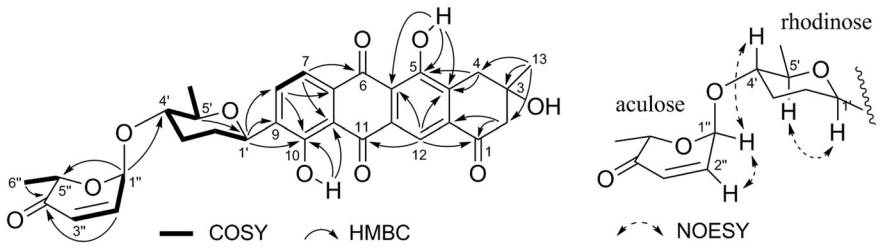

Fig. 2 Key 2D NMR correlations for **1**

suggested by the maximal UV absorption at 210, 265, and 471 nm, the conjugated carbonyl ^{13}C signals at δ 188.2 and 187.7, as well as the significantly downfield shifted hydroxyl ^{1}H signals at 13.14 and 13.08 due to OH bonding [13]. Analysis of HMBC correlations (Fig. 2) from H-12 to C-1, C-11, C-4a, and C-5a, H-13 to C-2, C-3, and C-4, H-4 to C-4a and C-5, and H-2 to C-1 and C-12a, along with three aromatic protons (δ_H 7.88, d, 7.8 Hz; 7.93, d, 7.8 Hz; 8.49, s), revealed that **1** had a linear tetracyclic anthraquinone aglycone as grincamycins E [14] and G [15]. Meanwhile, two doublet methyl signals (δ_H 1.38 & 1.40) and two anomeric methine signals (δ_H 4.85 & 5.34; δ_C 73.3 & 95.1) indicated the presence of two sugars in **1**. The ^{1}H–^{1}H COSY correlations across H-1' to H_3-6' spin coupling fragment and HMBC correlation from H-5' to C-1' revealed a rhodinose moiety, while ^{1}H–^{1}H COSY correlations of H-2" with H-1" and H-3", and H-5" with H_3-6", as well as HMBC correlations from H-2" and H_3-6" to C-4", and H-1" to C-5", enabled the assembly of an aculose moiety (Fig. 2). The HMBC correlation from H-1" to C-4' established the disaccharide fragment as aculose-(1 → 4)-rhodinose, while the *C*-glycosyl bond between C-9 and C-1' was supported by the HMBC correlations from H-1' to C-8, C-9, and C-10. The coupling constants of $J_{1',2'}$ (11.1 Hz) and $J_{1'',2''}$ (3.5 Hz) implied the relative configurations of the two anomeric carbons were *β* for rhodinose and *α* for aculose, respectively [12]. The NOESY correlations from H-1′ to H-5′ and H-1″ to H-4′ further confirmed the relative configurations of the disaccharide part as shown (Fig. 2). The configuration of C-3 was considered to be consistent with that of N05WA963C [13] on the basis of excellent NMR data comparison, which was further supported by the proposed biosynthetic relation with the known co-metabolites as described later. Although aculose and rhodinose are usual sugar moieties in anthraquinone family, rhodinosyl *C*-glycoside at C-9 was reported for the first time.

Grincamycin M (**2**) was obtained as a yellow powder, and the molecular formula of $C_{32}H_{32}O_{11}$ was deduced from HR-ESIMS analysis (*m/z* 593.2026 $[M + H]^+$, calcd for 593.2017) and NMR data. The ^{1}H and ^{13}C NMR data (Table 1) of **2** showed high similarity to those of **5** with the only difference attributable to the appearance of a methoxy group (δ_H 4.04, δ_C 56.6) in **2** instead of the aromatic proton (H-5) in **5**, which was further confirmed by the remarkably

Table 1 ^{1}H (600 MHz) and 13C (150 MHz) NMR data for compounds **1** and **2** in $CDCl_3$

Pos.	**1**		Pos.	**2**	
	δ_C, type	δ_H, mult. (*J* in Hz)		δ_C, type	δ_H, mult. (*J* in Hz)
1	195.5, C		1	197.4, C	
2	51.8, CH_2	2.93, dd, 16.2, 2.0 2.81, d, 16.2	2	53.7, CH_2	3.13, d, 13.9 2.97, dd, 13.9, 1.4
3	71.4, C		3	72.7, C	
4	37.2, CH_2	3.38, dd, 18.2, 2.0 3.06, d, 18.2	4	37.8, CH_2	3.27, dd, 18.0, 1.4 2.90, d, 18.0
4a	137.5, C		4a	128.6, C	
5	161.6, C		5	160.8, C	
5a	117.6, C		6	108.2, CH	7.73, s
6	188.2, CH		6a	137.3, C	
6a	131.7, C		7	188.3, C	
7	119.8, CH	7.88, d, 7.8	7a	115.0, C	
8	133.5, CH	7.93, d, 7.8	8	158.3, C	
9	139.9, C		9	136.0, C	
10	159.5, C		10	134.0, CH	7.88, d, 7.8
10a	115.6, C		11	119.8, CH	7.70, d, 7.8
11	187.7, C		11a	134.2, C	
11a	131.3, C		12	181.9, C	
12	117.0, CH	8.49, s	12a	135.3, C	
12a	137.2, C		12b	137.8, C	
13	30.2, CH_3	1.55, s	13	30.8, CH_3	1.53, s
			OCH_3	56.6, CH_3	4.04, s
1'	73.3, CH	4.85, brd, 11.1	1'	71.6, CH	4.98, dd, 11.1, 1.6
2'	31.8[a], CH_2	2.31, m 1.50, m	2'	36.8, CH_2	2.46, ddd, 12.7, 4.5, 2.0 1.54, m
3'	31.7[a], CH_2	2.34, m 1.85, m	3'	77.4, CH	3.82, ddd, 11.5, 9.1, 4.5
4'	81.0, CH	3.44, ddd, 10.8, 9.2, 4.6	4'	74.71[b], CH	3.51, dd, 9.1, 9.0
5'	77.3, CH	3.58, dq, 9.2, 6.1	5'	74.68[b], CH	3.58, dq, 9.0, 6.0
6'	18.7, CH_3	1.38, d, 6.1	6'	17.7, CH_3	1.41, d, 6.0
1"	95.1, CH	5.34, d, 3.5	1"	91.6, CH	5.18, d, 2.9
2"	143.1, CH	6.84, dd, 10.2, 3.5	2"	71.2, CH	4.34, m
3"	127.5, CH	6.11, d, 10.2	3"	40.1, CH_2	2.69, dd, 17.4, 3.6 2.62, dd, 17.4, 2.8
4"	197.0, C		4"	207.9, C	
5"	70.6, CH	4.62, q, 6.8	5"	77.9, CH	4.75, q, 6.7
6"	15.3, CH_3	1.40, d, 6.8	6"	16.3, CH_3	1.38, d, 6.7
5-OH		13.14, s			
10-OH		13.08, s			

[a,b]Interchangeable assignments

downfield shifted C-5 signal (δ_C 160.8) and the HMBC correlations from the methoxy protons and H-4 to C-5 (Fig. 3). It is also worth to note that H_2-4 in **5** was resolved as a singlet signal while geminal coupling was observed for H_2-4 in **2**, which could be caused by the change of chemical environment around H_2-4 (Supplementary material, Table S1). Moreover, the structure and C-3 configuration was determined by the consistent NMR data of **2** with **5** and with N05WA963A [13] which had the same aglycone as **2**, as well as biogenetic consideration (Fig. 4) [4].

Grincamycin N (**3**) was obtained as a dark-red powder with the UV maximal absorption at 265 and 497 nm. The molecular formula of **3** was suggested as $C_{31}H_{28}O_{10}$ according to the HR-ESIMS ion at *m/z* 559.1600 ($[M-H]^-$, calcd for $C_{31}H_{27}O_{10}$, 559.1610). Detailed analysis of ^{1}H and ^{13}C NNR data (Table 2) of **3** implied a linear *C*-glycosylated tetracenequinone skeleton as galtamycin B [16], while the only difference was attributable to the disaccharide side chain at C-9. As with **2**, the sugar moiety of **3** was also assigned to be an α-cinerulose B-(1 → 4, 2 → 3)-β-olivose unit based on decent comparison between the NMR data of the two co-metabolites, which was further corroborated by careful examination of 2D NMR correlations (Supplementary material, Figs. S19–S22). Particularly, the location of 10-OH was established by its HMBC correlations to C-9, C-10 and C-10a. Although no HMBC correlations of 5-OH were observed, its dramatic downfield chemical shift (δ_H 15.06, brs), due to intramolecular hydrogen bonding with C-6 ketone, enabled its assignment as shown. The structure of **3** was thus characterized.

With seven angucycline analogs (**1**–**7**) in hand, we were able to propose a common biogenesis for these co-metabolites (Fig. 4). These angucyclines, belonging to the polyketide family, were apparently originated from the acetate biosynthetic pathway. The key intermediate involved could be the well-known UWM6 as clearly described previously [17]. A shunt product tetrangomycin from UWM6 [17] would yield moromycin (**5**) upon glycosylation and also produce **2** via methoxylation and glycosylation, while fridamycin D (**6**) could be obtained from tetrangomycin by Baeyer–Villiger oxidation, hydrolysis and

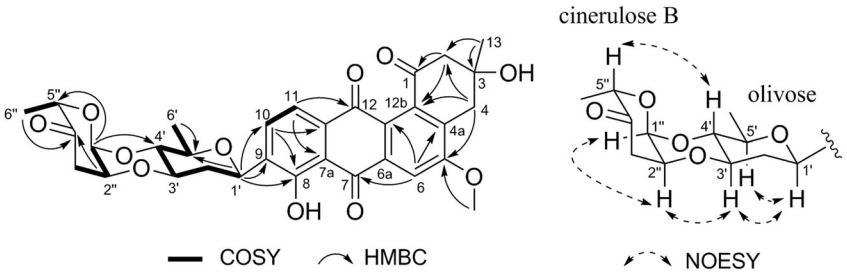

Fig. 3 Key 2D NMR correlations for **2**

glycosylation. Rabelomycin (**4**) could be easily produced from UWM6 through simple dehydration and isomerization, and a putative intermediate (**I**) from UWM6 [17] would afford saquayamycin B1 (**7**) via addition of the sugar moiety. Another important shunt intermediate (**II**) could be furnished from UWM6 as reported previously [18], and compounds **1** and **3** would derive from (**II**) via glycosylation and aromatization followed by glycosylation, respectively.

Compounds **1**–**9** were screened against a panel of human cancer cell lines A549, H157, MCF7, MDA-MB-231, and HepG2, and all the isolates exhibited significant cytotoxicity with IC_{50} values ranging from 0.09 nM to 17.30 μM (Table 3). Compounds **1**–**5** and **8**–**9** were also evaluated for their antimicrobial activity against two gram-positive strains *Mycobacterium smegmatis* ATCC 607 and *Staphylococcus aureus* ATCC 25923, two gram-negative strains *Escherichia coli* ATCC 8739 and *Pseudomonas aeruginosa* ATCC 9027 and a fungus *Candida albicans* ATCC10231 (**6** and **7** were not tested owing to limited samples). Only compounds **4**, **8**, and **9** showed antibacterial activity against the two gram-positive strains *M. smegmatis* and *S. aureus* with IC_{50} values from 0.12 to 23.1 μM (Table 3).

Experimental section

General experimental procedures

NMR spectra were acquired on a Bruker Avance DRX600 NMR spectrometer (Bruker BioSpin AG, Fällanden, Switzerland) with residual solvent peaks as references ($CDCl_3$: δ_H 7.26, δ_C 77.16; pyridine-d_5: δ_H 8.71/7.55/7.18, δ_C 149.7/135.3/123.3). Optical rotations were measured on a Rudolph VI polarimeter (Rudolph Research Analytical, Hackettstown, USA) with a 10 cm length cell. UV spectra were obtained on a Shimadzu UV-2600 spectrophotometer (Shimadzu, Kyoto, Japan) with 1 cm pathway cell. HR-ESIMS data were acquired on an Agilent 6545 Q-TOF mass spectrometer (Agilent Technologies Inc., Waldbronn, Germany). Semi-preparative HPLC separations were carried out on an Agilent 1260 series (Agilent Technologies Inc., Waldbronn, Germany) using an Agilent Zorbax SB-C_{18} column (250×9.4 mm, 5 μm). Column chromatography (CC) was performed on Silica gel (200–300 mesh, Yantai Jiangyou Silica Gel Development Co., Yantai, China) and Sephadex LH-20 gel (GE Healthcare Bio-Sciences AB, Uppsala, Sweden). All solvents used for CC were of analytical grade (Tianjin Fuyu Fine Chemical Co. Ltd., Tianjin, China) and solvents used for HPLC were of HPLC grade (Oceanpak Alexative Chemical Ltd., Goteborg, Sweden).

Biological material

The actinomycete XZHG99T strain was isolated from a soil sample collected from Color desert, Dengpa District, Tibet Autonomous Region, China (29°66′ N, 84°55′ E). Comparison of the 16S rRNA sequence of XZHG99T strain with the data from GenBank database (98.42% similarity to *S. albiflavescens* KCTC 29196T and 98.14% similarity to *S. rungchingensis* KCTC 29503T), in combination with the morphological traits, revealed that it might represent a new species of the genus *Streptomyces*. The BLAST sequenced data had been deposited at GenBank (accession no. MG272441). The strain was deposited in CGMCC center, Institute of Microbiology, Chinese Academy of Sciences.

Fermentation and extraction

Although the *Streptomyces* sp. XZHG99T showed well inhibitory activity against *Staphylococcus aureu*, HPLC analysis of the crude extract cultured in DS medium showed poor compound diversity. Therefore, different agents were tried to enrich the metabolites from *Streptomyces* sp. XZHG99T, and DS medium with 3% sea salt was found to yield more metabolites with better antimicrobial activity (Figs. S26–S27).

The *Streptomyces* sp. XZHG99T was inoculated in 500 mL Erlenmeyer flasks containing 150 mL DS medium (0.5% soluble starch, 0.03% casein, 0.2% KNO_3, 0.2% K_2HPO_4 $3H_2O$, 0.005% $MgSO_4$ $7H_2O$, 0.002% $CaCO_3$, and 0.001% $FeSO_4$ $7H_2O$) at 30 °C on a rotary shaker at 140 rpm for 2 days as seed cultures. Then each of the seed cultures (10 mL) was inoculated into autoclaved 500 mL Erlenmeyer flasks containing 150 mL DS medium described

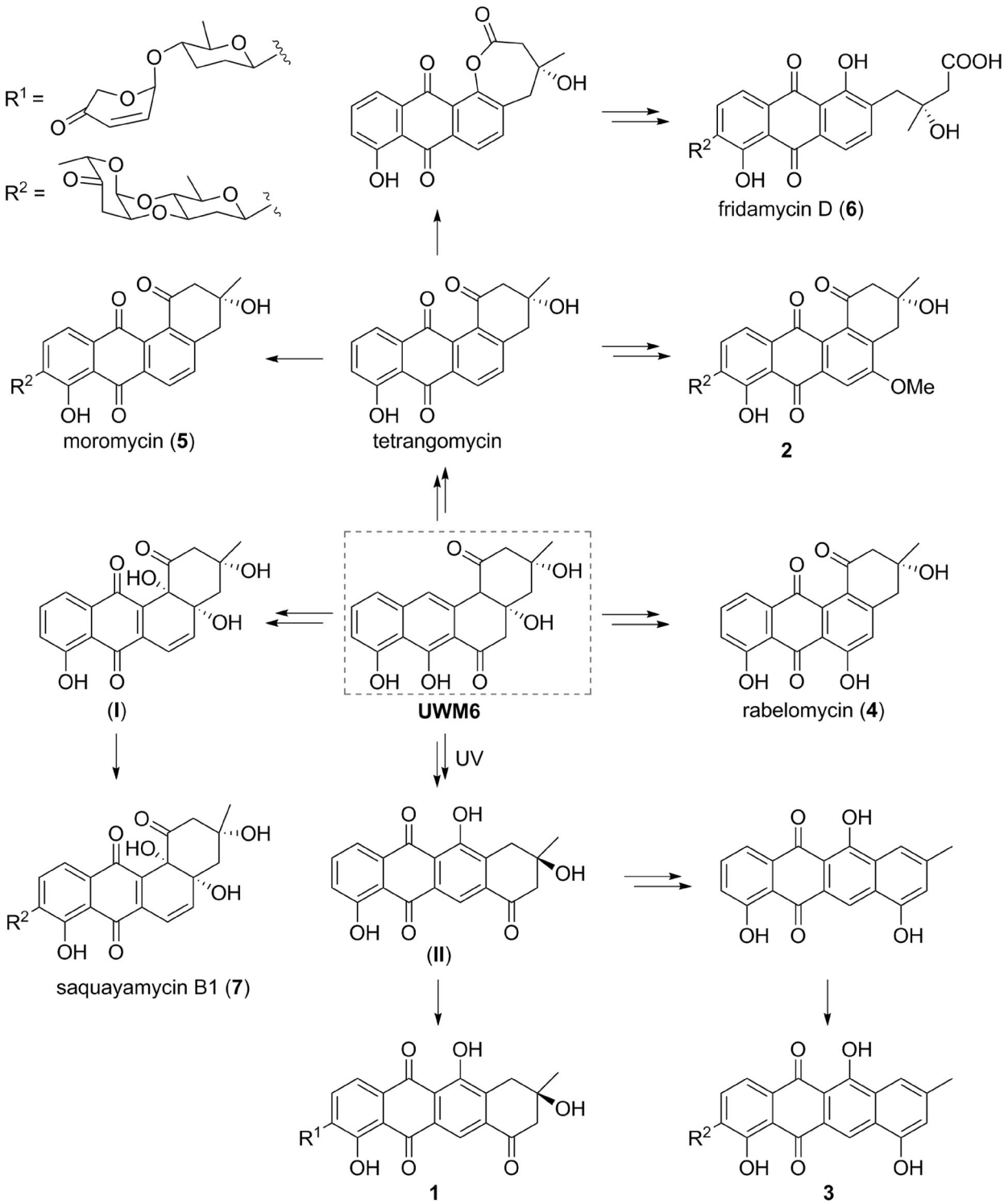

Fig. 4 Putative biosynthetic pathway for **1–7**

above but containing 3% sea salt. The flasks were incubated at 30 °C for 7 days on a rotary shaker (140 rpm).

The total 40 L fermentation broth was harvested and filtered to give filtrate and mycelia. The filtrate was extracted with an equal volume EtOAc three times, while the mycelia were extracted with 3.0 L 80% acetone three times. The acetone extract was evaporated under reduced pressure to afford an aqueous solution which was then

Table 2 ^{1}H (600 MHz) and ^{13}C (150 MHz) NMR data for compound **3** in pyridine-d_5

Pos.	δ_C, type	δ_H, mult. (*J* in Hz)
1	157.5, C	
2	116.8, CH	7.22, s
3	142.2, C	
4	115.2, CH	7.97, s
4a	129.5, C	
5	163.5, C	
5a	109.7, C	
6	187.1, C	
6a	133.3, C	
7	118.7, CH	8.09, d, 7.9
8	133.3, CH	8.06, d, 7.9
9	137.1, C	
10	159.3, C	
10a	117.0, C	
11	188.2, C	
11a	126.1, C	
12	118.1, CH	9.28, s
12a	125.7, C	
13	21.9, CH_3	2.36, s
1'	71.7, CH	5.16, dd, 11.1, 1.7
2'	36.6, CH_2	1.78, m 2.61, m
3'	76.8, CH	3.85, m
4'	74.5, CH	3.66, m
5'	74.6, CH	3.86, m
6'	17.6, CH_3	1.49, d, 6.1
1"	91.6, CH	5.44, d, 2.8
2"	71.6, CH	4.41, m
3"	40.2, CH_2	2.89, dd, 17.4, 2.7 2.80, dd, 17.4, 3.6
4"	208.2, C	
5"	77.8, CH	5.08, q, 6.7
6"	16.4, CH_3	1.44, d, 6.7
5-OH		15.06
10-OH		13.95

extracted with EtOAc. The two organic layers were combined and dried to give a crude gum (9.8 g).

Isolation and purification

The whole EtOAc extract (9.8 g) was fractionated by a silica gel CC eluting with step gradient CH_2Cl_2-MeOH (v/v 100:0 to 0:100) to give seven fractions (Fr.1–Fr.7) based on TLC and HPLC analysis. Fr.3 (1.9 g) was repeatedly separated by silica gel CC with step gradient CH_2Cl_2-$(CH_3)_2CO$ (v/v 100:0 to 0:100) and divided into six subfractions (Fr.3-1–Fr.3-6). Fr.3-3 (221.4 mg) was subjected to MPLC with an ODS column eluting with step gradient MeOH-H_2O (v/v 20:80 to 0:100) to give three subfractions (Fr.3-3-1–Fr.3-3-3) and Fr.3-3-2 (36.8 mg) was further purified by HPLC eluting with MeOH-H_2O-AcOH (v/v/v 95:5:0.05, 3.0 mL min^{-1}) to yield **3** (t_R = 13.6 min, 5.2 mg); Fr.3-4 (150.2 mg) was divided by Sephadex LH-20 CC eluting with MeOH-CH_2Cl_2 (v/v 1:1) and then purified by HPLC eluting with MeCN-H_2O (v/v 70:30, 3.0 mL min^{-1}) to afford **1** (t_R = 27.3 min, 2.3 mg); Fr.3-5 (314.8 mg) was also fractionated by Sephadex LH-20 CC eluting with MeOH-CH_2Cl_2 (v/v 1:1) to obtain four subfractions (Fr.3-5-1–Fr.3-5-4) and Fr.3-5-2 (56.8 mg) was purified by HPLC eluting with MeOH-H_2O (v/v 77:23, 3.0 mL min^{-1}) to yield **7** (t_R = 8.3 min, 0.6 mg), **5** (t_R = 11.5 min, 1.3 mg), and **2** (t_R = 14.6 min, 2.9 mg), while Fr.3-5-4 (9.3 mg) was purified by HPLC eluting with MeOH-H_2O-AcOH (v/v/v 68:32:0.05, 3.0 mL min^{-1}) to yield **4** (t_R = 16.6 min, 2.2 mg). Fr.5 (567.4 mg) was first subjected to Sephadex LH-20 CC eluting with MeOH and then isolated by HPLC eluting with MeOH-H_2O-AcOH (v/v/v 85:15:0.05, 3.0 mL min^{-1}) to yield **8** (t_R = 11.8 min, 7.2 mg) and **9** (t_R = 14.9 min, 20.2 mg). Fr.6-2 (7.5 mg) obtained from Fr.6 (189.1 mg) via Sephadex LH-20 CC eluting with MeOH was further purified by HPLC eluting with MeOH-H_2O-AcOH (v/v/v 85:15:0.05, 3.0 mL min^{-1}) to give **6** (t_R = 16.3 min, 0.8 mg).

Table 3 Biological activity of compounds **1**–**9** (IC_{50}, μM)

Compound	Cytotoxicity					Antimicrobial activity	
	A549	H157	MCF7	MDA-MB-231	HepG2	MS	SA
1	1.92	2.20	7.24	4.67	3.71	>50	>50
2	3.10	2.82	2.81	2.14	9.12	>50	>50
3	9.01	2.11	6.76	5.75	8.12	>50	>50
4	1.81	1.52	4.36	6.46	9.54	23.10	11.29
5	1.80	1.94	13.80	6.16	3.63	>50	>50
6	4.33	3.80	3.38	4.37	17.30	NT	NT
7	6.71	2.33	12.10	2.81	7.07	NT	NT
8	0.28 [a]	0.09[a]	3.01[a]	0.82[a]	0.12[a]	0.50	0.12
9	0.76 [a]	2.45[a]	6.16[a]	0.91[a]	0.41[a]	0.97	0.52
Vinorelbine	6.91	2.45	10.00	0.85	1.41	—	—
Penicillin	—	—	—	—	—	0.12	0.12

> 50 means the inhibition ratio tested at 50 μM was <50%

MS Mycobacterium smegmatis ATCC607, *SA Staphylococcus aureus* ATCC25923, *NT* not tested

[a]IC50 values in nM

*Grincamycin L (**1**).* Yellow powder; $[\alpha]^{21}_D$ 65.1 (*c* 0.1, $CHCl_3$); UV (MeOH) λ_{max} (log ε) 210 (3.77), 265 (3.25), 471 (2.45) nm; ^{1}H and ^{13}C NMR data, Table 1; IR (KBr) ν_{max} 3457, 2931, 1698, 1636, 1420, 1237, 1045, 797 cm^{-1};

(–)-HR-ESIMS *m/z* $[M-H]^-$ 561.1764 (calcd for $C_{31}H_{29}O_{10}$, 561.1766).

*Grincamycin M (**2**)*. Pale yellow powder; $[\alpha]^{21}_D$ 4.5 (*c* 0.18, $CHCl_3$); UV (MeOH) λ_{max} (log ε) 223 (3.64), 274 (3.00), 390 (2.02) nm; ^1H and ^{13}C NMR data, Table 1; IR (KBr) ν_{max} 3448, 1698, 1627, 1556, 1429, 1362, 1278, 1107 cm^{-1}; (+)-HR-ESIMS *m/z* 593.2026 $[M+H]^+$ (calcd for $C_{32}H_{33}O_{11}$, 593.2017).

*Grincamycin N (**3**)*. Dark-red powder; $[\alpha]^{21}_D$ 12.5 (*c* 0.04, MeOH); UV (MeOH) λ_{max} (log ε) 265 (5.04), 497.0 (4.40) nm; ^1H and ^{13}C NMR data, Table 2; IR (KBr) ν_{max} 3448, 2931, 1733, 1614, 1575, 1435, 1390, 1260, 1097, 1027, 905 cm^{-1}; (–)-HR-ESIMS *m/z* 559.1600 $[M-H]^-$ (calcd for $C_{31}H_{27}O_{10}$, 559.1610).

Antimicrobial assay

The antimicrobial activity of compounds **1**–**5** and **8**–**9** was assayed against the gram-positive strains *M. smegmatis* ATCC 607 and *S. aureus* ATCC 25923, gram-negative strains *E. coli* ATCC 8739 and *P. aeruginosa* ATCC 9027 and fungus *C. albicans* ATCC10231, by the two-fold serial dilution method in 96-well microplates as described previously [19]. Penicillin was used as positive control in the current assay.

Cytotoxic assay

The cytotoxicity of compounds **1**–**9** was evaluated toward A549, H157, MCF7, MDA-MB-231, and HepG2 cell lines using the SRB method as described previously [20], and vinorelbine was used as positive control.

Acknowledgements We acknowledge the financial support from National Natural Science Foundation of China (Nos. 41506148 & 81673527), Natural Science Foundation of Shandong Province (Nos. BS2015HZ005 & JQ201721), Primary Research and Development Plan of Shandong Province (2016GSF121018), Shandong Provincial Natural Science Joint Found with Universities and Scientific Research Institutes (ZR2018LC001), the Young Taishan Scholars Program (tsqn20161037), and Shandong Talents Team Cultivation Plan of University Preponderant Discipline (No. 10027).

Compliance with ethical standards

Conflict of interest The authors declare that they have no conflict of interest.

References

1. O'Neill J. Review on Antimicrobial Resistance. Antimicrobial Resistance: tacking a crisis for the health and wealth of nations. 2014.
2. Subramani R, Aalbersberg W. Marine actinomycetes: an ongoing source of novel bioactive metabolites. Microbiol Res. 2012;167:571–80.
3. Bentley SD et al. Complete genome sequence of the model actinomycete *Streptomyces coelicolor* A3(2). Nature. 2002;417:141–7.
4. Rohr J, Thiericke R. Angucycline group antibiotics. Nat Prod Rep. 1992;9:103–37.
5. Wang D et al. Identification, bioactivity, and productivity of actinomycins from the marine-derived *Streptomyces heliomycini*. Front Microbiol. 2017;8:1147.
6. Rathod BB, Korasapati R, Sripadi P, Shetty PR. Novel actinomycin group compound from newly isolated *Streptomyces* sp. RAB12: isolation, characterization, and evaluation of antimicrobial potential. Appl Microbiol Biot. 2018;10:1241–50.
7. Kharel MK et al. Angucyclines: biosynthesis, mode-of-action, new natural products, and synthesis. Nat Prod Rep. 2012;29:264–325.
8. Liu WC et al. Isolation, characterization, and structure of rabelomycin, a new antibiotic. J Antibiot. 1970;23:437–41.
9. Zhu L et al. Identification of the function of gene *lndM2* encoding a bifunctional oxygenase-reductase involved in the biosynthesis of the antitumor antibiotic landomycin E by *Streptomyces globisporus*1912 supports the originally assigned structure for landomycinone. J Org Chem. 2005;70:631–8.
10. Abdelfattah MS, Kharel MK, Hitron JA, Baig I, Rohr J. Moromycins A and B, isolation and structure elucidation of *C*-glycosylangucycline-type antibiotics from *Streptomyces* sp. KY002. J Nat Prod. 2008;71:1569–73.
11. Maskey RP, Helmke E, Laatsch H. Himalomycin A and B: isolation and structure elucidation of new fridamycin type antibiotics from a marine *Streptomyces* isolate. J Antibiot. 2003;56:942–9.
12. Shaaban KA, Ahmed TA, Leggas M, Rohr J. Saquayamycins G-K cytotoxic angucyclines from *Streptomyces* sp. including two analogues bearing the aminosugar rednose. J Nat Prod. 2012;75:1383–92.
13. Ren X et al. Three novel members of angucycline group from *Streptomyces* sp. N05WA963. J Antibiot. 2011;64:339–43.
14. Huang H et al. Cytotoxic angucycline class glycosides from the deep sea actinomycete *Streptomyces lusitanus* SCSIO LR32. J Nat Prod. 2012;75:202–8.
15. Zhu X et al. Cytotoxic rearranged angucycline glycosides from deep sea-derived *Streptomyces lusitanus* SCSIO LR32. J Antibiot. 2017;70:819–22.
16. Antal N et al. Retymicin, galtamycin B, saquayamycin Z and ribofuranosyllumichrome, novel secondary metabolites from *Micromonospora* sp. Tü 6368 II. Structure elucidation. J Antibiot. 2005;58:103–10.
17. Salem SM, Weidenbach S, Rohr J. Two cooperative glycosyltransferases are responsible for the sugar diversity of saquayamycins isolated from *Streptomyces* sp. KY 40-1. ACS Chem Biol. 2017;12:2529–34.
18. Zhang Y et al. Identification of the grincamycin gene cluster unveils divergent roles for GcnQ in different hosts, tailoring the l-Rhodinose moiety. Org Lett. 2013;15:3254–7.
19. Wang P et al. Phenolic bisabolane sesquiterpenoids from a Thai mangrove endophytic fungus, *Aspergillus* sp. xy02. Fitoterapia. 2018;127:322–7.
20. Ge D et al. Phosphorylation and nuclear translocation of integrin β4 induced by a chemical small molecule contribute to apoptosis in vascular endothelial cells. Apoptosis. 2013;18:1120–31.